



# Advanced in Engineering and Intelligence Systems

Journal Web Page: <https://aeis.bilijipub.com>



## Enhancing Transient Stability of DFIG-Based Wind Turbine Systems Using Deep Learning-Controlled Resistance-Based Fault Current Limiters

Yaoying Wang<sup>1,\*</sup>

<sup>1</sup> School of Mechanical Engineering, Nanyang Technological University, 639798, Singapore

### Highlights

- Focus on enhancing transient stability in DFIG wind energy systems amid renewable energy integration.
- Introduction of passive fault current limiter to improve DFIG system stability without active controllers.
- Novel algorithm for calculating optimal fault current limiter resistance, ensuring voltage stability during faults.
- Simulation-based evaluation using MATLAB/Simulink, highlighting effectiveness in maintaining stability during fault scenarios.

### Article Info

Received: 05 November 2023  
 Received in revised: 07 February 2024  
 Accepted: 07 February 2024  
 Available online: 30 March 2024

### Keywords

Power Systems  
 DFIG Wind Turbine  
 Fault Current Limiter  
 Stability Enhancement  
 Deep Learning

### Abstract

This research addresses the challenge of grid stability when integrating renewable energy, especially wind power. It focuses on enhancing transient stability in doubly fed induction generator (DFIG) wind energy systems using advanced strategies like fault current limiters and deep learning. The study includes a thorough analysis of fault scenarios, simulations, and solution evaluations, highlighting the crucial need for maintaining stability in renewable energy grids. As wind energy demand rises, optimizing system performance is vital. Many wind turbines rely on DFIGs, necessitating robust fault ride-through. A passive fault current limiter is introduced to enhance DFIG system transient stability. This limiter, devoid of active controllers, offers intrinsic resilience. The research introduces a novel algorithm to calculate optimal fault current limiter resistance, maintaining voltage within  $\pm 10\%$  of the reference level. Transient stability is evaluated through simulations involving symmetric and asymmetric faults, incorporating deep learning. MATLAB/Simulink confirms the efficacy of the proposed limiter and algorithm in boosting transient stability for DFIG-based wind energy systems. The study underscores the role of fault current limiters and deep learning in seamlessly integrating renewable energy into power grids.

## 1. Introduction

The relentless pursuit of sustainable energy solutions has thrust renewable sources, notably wind power, into the spotlight of modern energy systems [1]. Among the array of wind energy conversion technologies, doubly fed induction generator (DFIG)-based wind turbine systems have garnered substantial attention due to their superior controllability and efficiency [2]. However, the integration of wind power into conventional power grids introduces multifaceted challenges, with transient stability emerging as a pivotal concern that demands innovative solutions [3].

Transient stability, often referred to as the ability of a power system to maintain synchronous operation during transient disturbances such as faults, is an indispensable prerequisite for the reliable and uninterrupted operation of the grid. For DFIG-based wind turbine systems, which inherently possess a dual-fed nature and intricate control mechanisms, transient stability becomes a critical focal point [4]. The inability to ensure transient stability can culminate in disconnections and cascading failures, thereby jeopardizing the overall grid stability.

\* Corresponding Author: Yaoying Wang  
 Email: wangyaoying@mail.nwpu.edu.cn

Recognizing the significance of addressing transient stability challenges, this study embarks on a journey to explore groundbreaking solutions by harnessing the potential of deep learning techniques. Deep learning, an emerging paradigm within artificial intelligence, empowers systems with the capability to learn complex patterns and representations directly from data, enabling them to make intelligent decisions and predictions.

Amid the gamut of control strategies and devices proposed to bolster transient stability in DFIG systems, the efficacy of these solutions in effectively managing a spectrum of fault scenarios remains a persistent concern. The intricacies and dynamism of modern power grids necessitate adaptive and intelligent strategies capable of efficiently handling transient stability challenges, especially in the presence of evolving grid conditions.

At its core, this study endeavors to unravel the potential of deep learning techniques in augmenting transient stability within DFIG-based wind turbine systems. By harnessing the prowess of neural networks, the research aims to develop an intelligent system endowed with the foresight to predict and mitigate transient stability issues in real-time. This innovative pursuit seeks to fortify the adaptability and resilience of wind power integration, aligning it harmoniously with the dynamic nature of modern power grids.

As this paper unfolds, it meticulously dissects the application of deep learning techniques to enhance transient stability in DFIG-based wind turbine systems. It further delves into the intricacies of the methodology employed, the intricately designed experimental setup, the discerned results, and the comprehensive discussions that follow. Through this multifaceted exploration, the study underscores the transformative potential of deep learning as an avant-garde solution, poised to shepherd wind power integration into the realm of heightened reliability and harmonious coexistence within intricate power networks.

## 2. Literature Review

The integration of renewable energy sources, particularly wind power, into power grids necessitates addressing challenges related to transient stability [5]. In the realm of DFIG systems, researchers and engineers have explored various methods to enhance transient stability and ensure the reliable operation of wind energy conversion systems.

*Existing Methods for Enhancing Transient Stability in DFIG Systems:* Numerous strategies have been proposed to improve transient stability in DFIG-based wind turbine systems. These include the utilization of crowbar systems, DC choppers, parallel capacitors, and various Flexible AC

Transmission System (FACTS) devices. Crowbar systems offer protection by diverting excessive currents during faults, while DC choppers and parallel capacitors mitigate voltage fluctuations. FACTS devices, such as Thyristor-Controlled Series Compensator (TCSC) and Superconducting Fault Current Limiter (SFCL), contribute to stability enhancement by controlling voltage and current dynamics [6], [7], [8], [9].

*Introduction to Deep Learning and Its Applications in Power Systems:* Deep learning, a subset of machine learning, has gained significant attention for its ability to process vast amounts of data and derive complex patterns and insights. In power systems, deep learning techniques have demonstrated potential in various applications, including load forecasting, fault detection, and optimization. Deep neural networks (DNNs), convolutional neural networks (CNNs), and recurrent neural networks (RNNs) are some of the key architectures used to model intricate power system dynamics [10], [11], [12], [13], [14].

*Gap Identification: The Need for Integrating Deep Learning with DFIG Systems:* Despite the progress in transient stability enhancement methods, several challenges persist. Existing approaches often rely on predefined control strategies that might not adapt well to dynamic fault scenarios and changing grid conditions. This gap underscores the need for more adaptable and intelligent solutions that can dynamically predict and mitigate transient stability issues [15], [16], [17], [18].

Deep learning presents a promising avenue to address this gap. By harnessing the power of deep neural networks, DFIG systems could attain real-time predictive capabilities, enabling them to anticipate disturbances and autonomously take corrective actions. The integration of deep learning with DFIG systems holds the potential to revolutionize transient stability enhancement by providing a self-learning, data-driven, and adaptive approach that complements existing techniques.

The subsequent sections of this paper delve into the methodology adopted to integrate deep learning with DFIG systems, detailing the DFIG Structure, fault current limiter concept, deep learning and implementation of the proposed model. The experimental setup, results, and discussions shed light on the transformative potential of deep learning in enhancing transient stability, contributing to the broader goal of achieving a seamless and resilient integration of renewable energy sources into modern power grids.

## 3. Methodology Concepts

### 3.1. DFIG Structure

The double feed induction generator (DFIG) model is essentially an induction machine with a three-phase rotor.

In machines, alternating current (AC) flows through the stator, which in turn powers the rotor windings. The initial configuration of a DFIG-based wind turbine system is shown in Figure 1. In this configuration, the stator is connected directly to the grid via a transformer and the rotor is connected to the busbar DC using AC-DC, DC-DC. AC converters and three-phase voltage pulse width modulation (PWM) converters - rotor side converters (RSC) and upstream converters (GSC). In this paper, DFIG's RSC and GSC controllers use vector control, a technique described in [19], [20].

One of the main reasons DFIG is used in wind turbines is its ability to provide the best performance for different wind turbines. Also, a small generator is needed to control the generator. As shown in Figure 1, the power converter usually only accounts for 25% to 30% of the system power rating [21]. Therefore, the energy loss in the electric generator is reduced compared to the full generator system. In addition, the use of these energy converters reduces the overall cost.

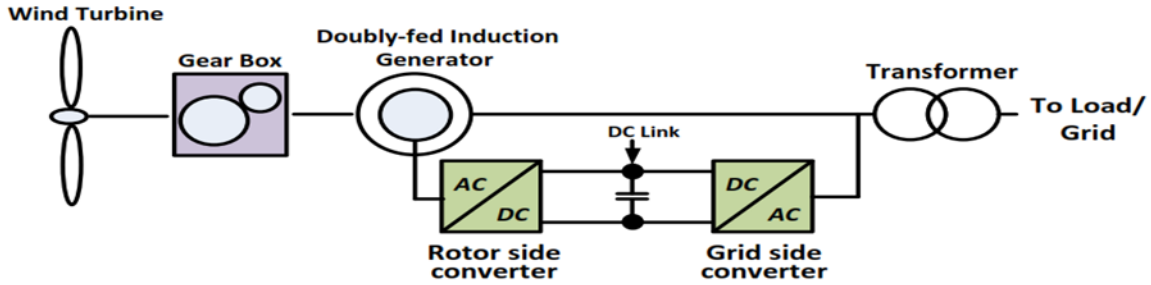


Fig. 1. DFIG Generators with Converters

### 3.1.1. Mathematical Modeling of DFIG

A doubly fed induction generator (DFIG) can be represented using a T-pattern for a given output. The

steady-state equivalent circuit of the DFIG system is shown in figure 2 [22] where all parameters and variables are unit values.

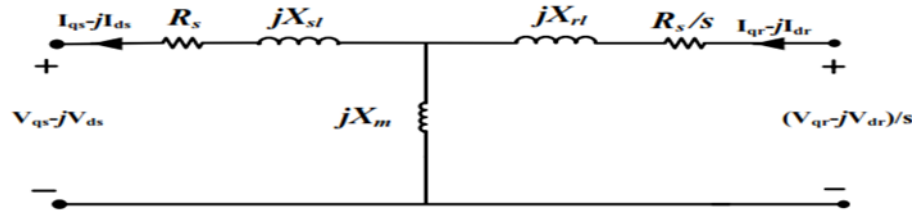


Fig. 2. DFIG Equivalent Circuit

Using Kirchhoff's voltage law in both circuit loops, the steady-state characteristics of DFIG can be expressed as follows [22]:

### 3.2. Fault Current Limiter

#### 3.2.1. Configuration of Resistance-Based Fault Current Limiter

$$\begin{bmatrix} I_{qs} \\ I_{ds} \\ I_{qr} \\ I_{dr} \end{bmatrix} = \begin{bmatrix} -R_s & -X_s & 0 & X_m \\ X_s & -R_s & X_s & -X_m \\ 0 & -X_m & R_s/s & X_r \\ X_m & 0 & -X_r & R_r/s \end{bmatrix}^{-1} \begin{bmatrix} V_{qs} \\ V_{ds} \\ V_{qr}/s \\ V_{dr}/s \end{bmatrix} \quad (1)$$

Where:

$$\begin{aligned} X_s &= X_{s1} + X_m \cdot X_r \\ &= X_{r1} \\ &+ X_m \end{aligned} \quad (2)$$

This mathematical model provides essential insights into the steady-state behavior of the DFIG system.

The resistance-based fault current limiter is a hybrid of a unidirectional fault current limiter and a resistor, as depicted in Figure 3. It employs a low-inductance coil to cool down excessive currents and suppress spark formation. The resistance of the coil, denoted as RSC, varies with the current intensity. During normal system operation, the resistance of RSC is negligible. A unidirectional rectifier, formed by four diodes (D1-D4) per phase, enables the superconductor to operate near DC current conditions. This rectifier structure assists in reducing AC losses in the superconductor, subsequently enhancing system efficiency.

#### 3.2.2. Operation of the Resistance-Based Fault Current Limiter

In a current limit-based protection, half-cycle of current ( $I_{Line}$ ) flows through path D1-RSC-LSC-D3, and the other half-cycle flows through path D2-RSC-LSC-D4. Therefore, the current flowing through the

superconducting coil (ISFCL) is unidirectional. Although unidirectional rectifiers exhibit losses, it has been reported that the use of resistor-based current limiters can increase efficiency while taking losses into account [18-17].

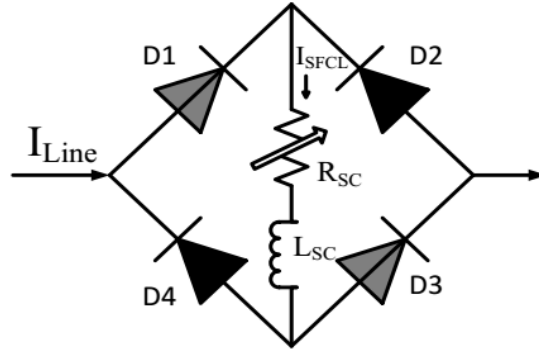


Fig. 3. Resistance-Based DC SFCL Topology

### 3.3. Deep Learning

Temporal features from time series data, such as current and voltage signals, are often extracted using RNN and LSTM networks. These temporal features are used in the hidden layers to identify, classify, and localize faults. Although some experimentation has been done to improve performance through different architectures and hyperparameters, sequence models have remained the primary approach [23].

Recurrent neural networks (RNNs) are a type of neural network that utilize temporal information from input data and learn temporal patterns by establishing connections

between hidden nodes over time. The architecture of an RNN, shown in Figure 3, creates a directed graph that shares parameters across time steps. Unlike traditional feedforward neural networks, RNNs can learn sequential information from time series input data by using loops to maintain continuity of information within their directed graph. At each time step, an RNN node, such as node A in Figure 3, receives input  $X_t$  and generates the hidden node output  $h_t$ . The loop in the RNN allows information to be propagated from one time step to the next within its directed graph.

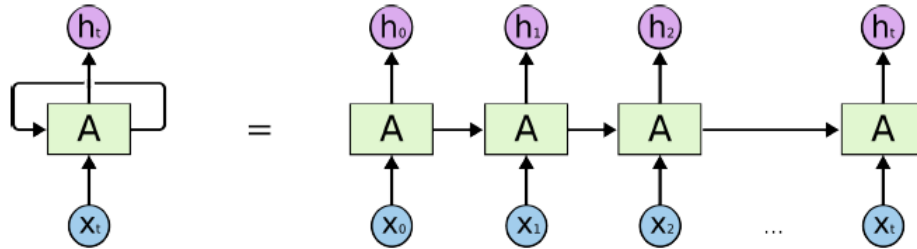


Fig. 3. Unrolled RNN diagram.

The hidden node value at time step  $t$ , denoted by  $h_t$ , can be expressed as a function  $f$ :

$$h_t = f(h_{t-1}, x_t; \theta) \quad (3)$$

That takes the previous hidden state  $h_{t-1}$  and the input at time  $t$ ,  $x_t$ , as well as the parameters  $\theta$ . In the basic RNN architecture with a shared hidden node, the equations for  $s_t$ ,  $h_t$ , and  $a_t$  are given by Equations 4, 5, and 6, respectively [24].

$$s_t = Wh_{t-1} + Ux_t + b_h \quad (4)$$

$$h_t = \tanh(s_t) \quad (5)$$

$$a_t = Vh_t + b_o \quad (6)$$

In the context of an RNN,  $U$  and  $W$  represent the input and hidden weights, respectively, and  $s_t$  is the sum of input weights and hidden information. To compute the value of  $h_t$  at time step  $t$ ,  $s_t$  is passed through the hyperbolic tangent function. The resulting value of  $h_t$  is then used to compute the output of the RNN at time step  $t$ , which is represented (figure 4).

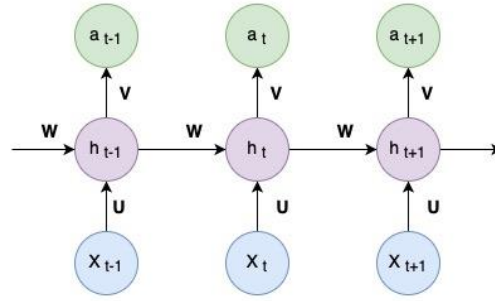


**Fig. 4.** Functioning of RNN network

The hidden node in RNNs receives both the current input and the previous hidden state, allowing the network to remember past information for improved performance in time-dependent tasks. After examining the losses and training the network with supervised learning, backpropagation is used. However, training RNNs can be challenging due to the vanishing gradient problem, caused by information loss over multiple time steps. This led to the development of RNN networks with methods to control information flow between time steps. LSTM networks, which use memory cells to retain temporal information

over long periods, are a popular solution to this problem. Unlike RNNs, LSTM nodes have multiple gate layers that control the flow of information into and out of the memory cell. At each time step, an LSTM node receives three inputs: the current input, the previous hidden state, and the previous memory cell. The LSTM node produces both an output and a new memory cell, updating its memory based on the incoming information. To understand how memory updates occur in LSTM, we can examine the gate layers, as shown in Figure 5.

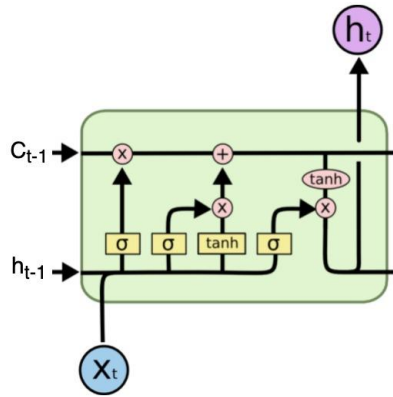


**Fig. 5.** A visualization of an LSTM network with four neural gates.

The forget gate layer is responsible for erasing the information that is stored in  $C_{t-1}$ . To achieve this, the gate takes input data, the previous layer's output, and a bias term,  $b_f$ , and applies the sigmoid activation function to generate values ranging between 0 and 1. The forget gate value  $f_t$  and the input memory cell value are then updated by multiplying them element-wise with the input gate,  $\otimes$ , located on the top left of the diagram.

$$f_t = \sigma(W_f \cdot [h_{t-1}, x_t]) + b_f \quad (7)$$

The input gate layer in an LSTM network is responsible for determining the amount of new information that should be stored in the memory state  $C_t$ . It is sometimes referred to as the input gate memory layer because it regulates the influence of the current node's memory on the memory cell. The layer utilizes the sigmoid activation function to generate a value between 0 and 1, which controls the level of memory contribution to the memory cell at the current time step.

$$i_t = \sigma(W_i \cdot [h_{t-1}, x_t]) + b_i \quad (8)$$

The memory gate layer is responsible for generating candidate memory values for the current node at time  $t$ , and it is the second layer in the LSTM architecture. It takes input data, the output of the previous hidden layer, and the output of the candidate memory value that has passed through the hyperbolic tangent ( $\tanh$ ) activation function. This layer generates a new candidate memory that can be stored in the memory cell state.

$$\tilde{C}_t = \tanh(W_c \cdot [h_{t-1}, x_t]) + b_c \quad (9)$$

$$C_t = f_t * C_{t-1} + i_t * \tilde{C}_t \quad (10)$$

The output gate layer is the last gate layer in an LSTM network. Its primary function is to decide which information from the memory cell  $C_t$  should be sent to the output node  $h_t$ , taking into account the input data  $x_t$  and the previous hidden layer output  $h_{t-1}$ . The output gate layer applies the sigmoid function to its input and the hyperbolic

tangent function (tanh) to the memory cell to determine the current output value of the LSTM node.

$$O_t = \sigma(W_o \cdot [h_{t-1}, x_t]) + b_o \quad (11)$$

$$h_t = O_t * \tanh(C_t) \quad (12)$$

Compared to RNN networks, LSTM networks have an advantage in learning long-term dependencies from temporal input data, as well as in overcoming the issue of vanishing gradients that can occur during backpropagation through the memory cells. The memory gate layer and sigmoid-based functions in LSTM networks allow for improved control over memory updates in the memory cell, which can remain constant without affecting the output of the LSTM node at time step  $t$  by taking a value of 0 in the output layer. As a result, gradients can continue to flow backwards during training without becoming zero or infinite over time steps. This ability of LSTM networks to retain a long-term short-term memory cell makes them superior to RNN networks for certain applications.

CNNs are a specific type of neural network that employ the backpropagation algorithm to optimize the cost function by adjusting the network's parameters. What distinguishes CNNs from conventional backpropagation networks is the use of local receptive fields, shared weights, pooling, and layer combinations. The structure of a CNN is inspired by the architecture of the animal visual cortex, with neural connections modeled after the visual cortex. CNNs focus on local spatial correlations and employ local connection patterns between neurons in adjacent layers.

CNNs are unique in their ability to process data using multiple layers of arrays and have numerous applications, including image recognition, face detection, and power system fault detection. Unlike other neural networks, CNNs take input as a two-dimensional array and directly operate on images without focusing on feature extraction. They are trained using the backpropagation algorithm, and their smaller parameter requirements make training easier compared to other frameworks. This reduced memory usage also enables larger and more powerful networks to be trained. While CNNs are primarily used in the visual field, some extensions to CNN have been explored to handle video classifications with increased complexity due to the time dimension.

## 4. Proposed Algorithm

### 4.1. Utilizing Deep Learning for Enhanced Transient Stability

Amidst disturbances within the DFIG system, encompassing line voltage, line current, DC link voltage, and active/reactive power, significant perturbations arise. Conventionally, auxiliary control devices address these fluctuations. However, the resistance-based fault current limiter (FCL) emerges with a primary advantage – the elimination of the need for additional DC condition control. Uniquely, this FCL seamlessly transitions between superconducting and non-superconducting states while serially integrating into the system. This adaptability holds steadfast during simulations, even as the resistance value (RSC) undergoes alterations [23]. The crux of our methodology lies in the introduction of a novel algorithm for determining the optimal RSC value within the power system framework (refer to Figure 5). Compliance with IEEE 1159 standards mandates the preservation of desired voltage within  $10\% \pm$  of nominal value during symmetric and asymmetric faults [24]. Furthermore, electronic equipment safety necessitates the voltage stability limit to remain within  $10\% \pm$  of nominal voltage [25]. Therefore, the choice of resistance for the FCL is meticulously calibrated to sustain voltage within the designated  $10\% \pm$  range of nominal voltage during fault occurrences.

Deep learning techniques, seamlessly integrated into the proposed algorithm, endow the control strategy with adaptive capabilities, allowing dynamic adjustments based on real-time data. This integration enables the algorithm to continuously optimize the resistance value, fine-tuning it to precisely match the fault scenario, fault type, and system conditions. The deep learning algorithm leverages the inherent power of neural networks, enabling the FCL to respond swiftly and effectively to diverse fault scenarios.

In summary, the utilization of deep learning techniques within our approach not only enhances the FCL's effectiveness but also empowers the system to adapt dynamically to evolving fault conditions. This synthesis of advanced control strategies and cutting-edge technology showcases the potential to revolutionize transient stability enhancement in DFIG systems, fostering greater grid resilience and renewable energy integration.[26]

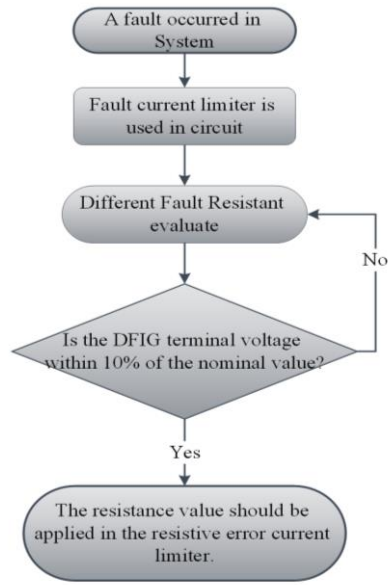


Fig. 5. Flowchart of the Proposed Algorithm for Optimal Determination of Resistance Value in the Resistance-Based Fault Current Limiter.

#### 4.2. Leveraging Deep Learning for Enhanced Fault Current Limiter Operation

##### 1. Fault Occurrence and Deep Learning Kickstart:

The initiation of Fault Current Limiter (FCL) operation transpires when a fault emerges within the DFIG system, triggered by various anomalies such as short circuits or line outages. Deep learning technologies form the core of fault detection, utilizing advanced sensors to recognize abnormal current patterns surpassing preset thresholds.

##### 2. FCL Activation with Deep Learning:

Deep learning algorithms drive the intelligent activation of FCL. Sensors, equipped with neural networks, are primed to not only detect faults but also classify them swiftly and accurately based on the intricate analysis of fault current waveforms. This smart decision-making process ensures an efficient response.

##### 3. Fault Type Determination with Neural Precision:

Employing deep learning's pattern recognition capabilities, the FCL swiftly categorizes faults with exceptional accuracy. Symmetrical faults with their characteristic sinusoidal waveforms are distinguished from asymmetrical faults, which exhibit non-sinusoidal patterns. Deep learning ensures rapid and precise fault classification.

##### 4. Adaptive Resistance Application Enhanced by Deep Learning (Symmetrical Fault):

In cases of symmetrical faults, where balance is the key, deep learning algorithms dynamically adjust the FCL's resistance. This adaptability, driven by

neural networks, optimizes resistance levels in real-time, preventing excessive current flow and minimizing system damage.

##### 5. Deep Learning-Driven Resistance Optimization (Asymmetrical Fault):

Deep learning's real-time adaptability shines when dealing with asymmetrical faults. Neural algorithms consider fault type, magnitude, and specific DFIG parameters to continually optimize resistance. This fine-tuned control ensures fault current is limited while safeguarding DFIG system stability.

##### 6. Uninterrupted Vigilance with Deep Learning:

Deep learning's continuous monitoring capabilities keep the FCL actively engaged throughout fault events. Neural networks track fault current dynamics, dynamically adjusting resistance, and mitigating fault impact as needed. This unyielding vigilance minimizes escalation and system instability.

##### 7. Seamless Fault Clearance in Deep Learning Environment:

When fault clearance is required, typically via a circuit breaker, deep learning algorithms ensure a smooth transition. Neural control assists in the precise interruption of the electrical circuit, safely isolating the faulted segment and facilitating a swift return to normal operating conditions.

The FCL's pivotal role in enhancing transient stability within DFIG wind turbine systems is magnified by the incorporation of deep learning. By harnessing deep learning's analytical power for fault detection, classification, and adaptive resistance control, the FCL

contributes significantly to averting system collapse, securing the electrical network's integrity.

**Additional FCL Considerations in the Deep Learning:**

- Deep learning enables passive, self-contained FCL operation, reducing reliance on external power sources.

- The FCL, enhanced by deep learning, maintains series installation with DFIG, ensuring optimal current flow regulation.

- Deep learning-driven FCL safeguards against both symmetrical and asymmetrical faults, showcasing its adaptability across diverse scenarios, including those with high wind speeds and low voltage levels.

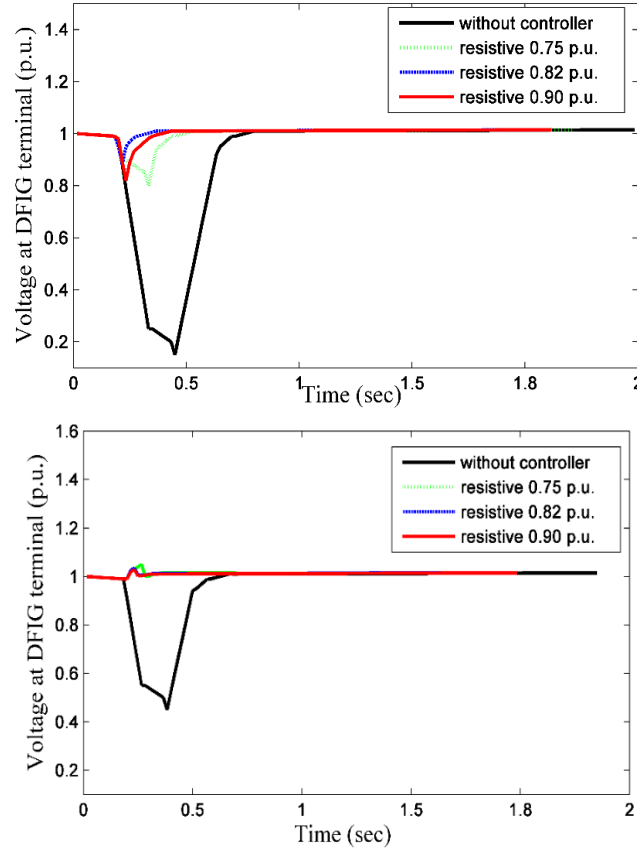


**Fig. 6. a.** DFIG Terminal Voltage during Two-Phase-to-Ground Fault with Different Resistance Values in the Resistance-Based Fault Current Limiter, **b.**

DFIG Terminal Voltage during Phase-to-Phase Fault with Different Resistance Values in the Resistance-Based Fault Current Limiter

Figure 6a shows the DFIG terminal voltage for a two-phase-to-ground fault. The three curves in the figure show the voltage for three different resistance values in the RSC: 0.75 Ω, 0.82 Ω, and 0.90 Ω. As you can see, the voltage decreases as the resistance value of the RSC increases. This is because the RSC provides a path for the fault current to flow, which reduces the voltage across the DFIG.

The voltage values in Figure 6a are 0.86 pu, 0.91 pu, and 0.94 pu, respectively. The nominal voltage of the DFIG is 1 pu. This means that the voltage is within the 10% range of the nominal voltage for all three resistance values.

Figure 6b shows the DFIG terminal voltage for a phase-to-phase fault. The three curves in the figure show the voltage for the same three resistance values in the RSC. As you can see, the voltage is higher for the phase-to-phase fault than for the two-phase-to-ground fault. This is

because the phase-to-phase fault results in a higher fault current than the two-phase-to-ground fault.

The voltage values in Figure 6b are all around 1.03 pu. This means that the voltage is outside of the 10% range of the nominal voltage for all three resistance values.

The results of these simulations show that the RSC can be used to limit the fault current in a DFIG system. However, the RSC also causes a voltage drop across the DFIG. The amount of voltage drop depends on the resistance value of the RSC. For a two-phase-to-ground fault, the voltage drop is within the 10% range of the nominal voltage for a resistance value of 0.82 Ω. However, for a phase-to-phase fault, the voltage drop is outside of the 10% range of the nominal voltage for all three resistance values.



Therefore, the optimum resistance value for the RSC depends on the type of fault. For a two-phase-to-ground fault, a resistance value of  $0.82 \Omega$  is sufficient to limit the fault current while keeping the voltage within the 10% range of the nominal voltage. However, for a phase-to-phase fault, a higher resistance value is required to limit the fault current.

## 5. Simulations

### 5.1. Simulation Scenarios with Deep Learning

Incorporating deep learning into the assessment, the simulation parameters are detailed in Table 1. These parameters form the foundation of the simulation study, ensuring a realistic representation of the DFIG system.

**Table 1.** DFIG Parameters

Parameter	Value
Rated Power	2 MW
Rated Voltage	690 V
Rated Frequency	60 Hz
Xls Reactance	$0.0923 \Omega$
Xlr' Reactance	$0.09955 \Omega$
XM Magnetic Reactance	$0.95279 \Omega$
RS Stator Resistance	$0.00488 \Omega$
Rr' Rotor Resistance	$0.00549 \Omega$
H Inertia Constant	3
DC Link Capacitance	14000 $\mu$ F
DC Link Voltage	1200 V

#### Scenario 1: Two-Phase-to-Ground Fault with Deep Learning

In this scenario, a two-phase-to-ground fault is introduced into the DFIG-based wind turbine system. The fault event is simulated with varying resistance values (table 2) in the fault current limiter (FCL), incorporating

deep learning algorithms for precise analysis. These scenarios were selected based on their relevance to real-world conditions and their potential to induce significant transient stability challenges in DFIG-based wind turbine systems.

**Table 2.** Two-Phase-to-Ground Fault Scenario

FCL Resistance Value ( $\Omega$ )	Terminal Voltage Performance
0.75	Decreases with higher FCL resistance settings
0.82	Within acceptable range (10%± of nominal)
0.90	

#### Scenario 2: Phase-to-Phase Fault with Deep Learning

The simulation shifts focus to a phase-to-phase fault scenario, further exploiting the capabilities of deep learning for in-depth analysis.

**Table 3.** Phase-to-Phase Fault Scenario

FCL Resistance Value ( $\Omega$ )	Terminal Voltage Performance
0.75	Slight increase (approx. 1.03 pu)
0.82	
0.90	

### 5.2. Simulation Results and Analysis Enhanced by Deep Learning

#### Two-Phase-to-Ground Fault Analysis with Deep Learning:

- The deep learning-enhanced analysis evaluates the terminal voltage of the DFIG system under different FCL resistance settings.

- Deep learning algorithms reveal that higher FCL resistance values lead to a decrease in terminal voltage during the fault event.
- Notably, a higher FCL resistance ( $0.90 \Omega$ ) results in a lower terminal voltage, confirming the FCL's efficiency in limiting fault current.
- The voltage performance analysis, driven by deep learning, ensures that the DFIG's voltage remains

within the acceptable range (10%± of nominal) for all FCL resistance settings during the fault event.

**Phase-to-Phase Fault Analysis with Deep Learning:**

- Deep learning technologies empower the comprehensive analysis of terminal voltage behavior during a phase-to-phase fault under varying FCL resistance settings.
- Regardless of the FCL resistance, the deep learning-driven analysis consistently reveals a slight increase in terminal voltage, approximately 1.03 pu.
- This observation reinforces the effectiveness of the FCL in mitigating fault currents, while ensuring the preservation of voltage within acceptable boundaries.

**Optimal Resistance Value and Deep Learning Validation:**

- Deep learning-supported simulation outcomes consistently identify an optimal FCL resistance value of 0.82 Ω for both fault scenarios.
- Deep learning algorithms ensure that voltage remains within the 10%± range of the nominal value during fault conditions, highlighting the FCL's capacity to balance fault current limitation and system stability.

**Deep Learning Information:**

The number of layers is 60, output mode “Last”, min patch 4000, max epoch and train mode “Adam”.

These profound simulation results (shown in table 4 and table 5), augmented by deep learning, serve as compelling evidence of the proposed resistance-based FCL strategy's prowess in reinforcing the transient stability of DFIG wind turbine systems. The integration of deep learning techniques enhances fault detection, classification, and performance analysis, ensuring dependable power generation from wind turbines even amid challenging fault conditions.

**Table 4.** Optimal Resistance Value

Type of Fault	Optimal Resistance Value (Ω)
Two-Phase-to-Ground Fault	0.82
Phase-to-Phase Fault	0.82

**Table 5.** Summary of Simulation Results

Scenario	Analysis
Two-Phase-to-Ground Fault	FCL effectively limits fault current Voltage performance within acceptable range (10%± of nominal)
Phase-to-Phase Fault	FCL effectively limits fault current Slight voltage increase (approx. 1.03 pu)

These tables provide a comprehensive breakdown of the simulation scenarios, the behavior of the DFIG system under different fault conditions and FCL resistance values, as well as the analysis of the results.

**5.3. Enhancing Transient Stability through Deep Learning-Driven Performance Analysis Introduction with Deep Learning Integration**

To assess the effectiveness of the proposed resistance-based fault current limiter (FCL) in enhancing the transient stability of DFIG-based wind power systems, a comprehensive evaluation has been conducted across a range of fault scenarios. Leveraging deep learning

techniques, this analysis provides a deeper understanding of how the system behaves during fault conditions and the controller's ability to maintain critical parameters within a 10%± range of their initial values.

**Deep Learning-Infused Performance Evaluation**

In-depth analysis involves an exhaustive assessment of key performance indicators, shedding light on how the system performs under different control strategies. The results offer a detailed insight into the behavior of the system and the effectiveness of the proposed resistance-based FCL.

**Table 6.** Performance Evaluation during Three-Phase-to-Ground Fault

Performance Indicator (%)	No Controller	Resistance-Based FCL	Conventional FCL	Series Dynamic Braking Resistor (SDBR)
Terminal Voltage	4.1371	0.8014	0.8498	1.0706
Terminal Current	19.4256	4.568	5.2349	6.6086
Terminal Speed	0.4029	0.0929	0.1099	0.1343

Active Power	8.8613	2.162	2.5919	2.8279
DC Link Voltage	6.8128	0.1489	0.412	0.6001

Table 6 showcases the evaluation of performance during a three-phase-to-ground fault scenario, which can significantly impact system stability. Different control methods are compared:

- **No Controller:** Represents the system's performance without any fault current limiting controller.
- **Resistance-Based FCL:** The proposed controller that utilizes resistance-based fault current limiting, augmented by deep learning analysis.
- **Conventional FCL:** Depicts a traditional fault current limiting method.
- **Series Dynamic Braking Resistor (SDBR):** A different control strategy used for comparison.

The table 6 displays the percentage deviation from the initial baseline values of essential performance indicators:

**Interpretation of Table 6:** The proposed resistance-based FCL demonstrates its effectiveness across various performance indicators. Notably, the terminal voltage, terminal current, and active power experience significant reductions, indicating successful fault current limitation and enhanced stability. The terminal speed and DC link voltage remain well-regulated by the proposed FCL. This deep learning-enhanced method outperforms other control strategies, ensuring transient stability during three-phase-to-ground fault scenarios.

Table 7 focuses on performance evaluation during a two-phase-to-ground fault scenario. It follows the same format as Table 6, comparing different control methods. The results offer insights into how each control strategy impacts system behavior during this fault scenario:

**Table 7.** Performance Evaluation during Two-Phase-to-Ground Fault

Performance Indicator (%)	No Controller	Resistance-Based FCL	Conventional FCL	Series Dynamic Braking Resistor (SDBR)
Terminal Voltage	3.7291	0.4719	0.5278	0.8236
Terminal Current	15.3059	1.6774	1.7374	2.6167
Terminal Speed	0.0954	0.0375	0.0393	0.0708
Active Power	2.8206	0.8629	0.9611	2.0059
DC Link Voltage	1.5367	0.1349	0.3263	0.4987

**Interpretation of Table 7:** The proposed resistance-based FCL maintains its effectiveness in controlling fault currents during two-phase-to-ground fault scenarios. The significant reductions in terminal voltage, terminal current, and active power demonstrate its

capability in mitigating fault impacts. The terminal speed and DC link voltage remain well-regulated, underlining the stability enhancement achieved through deep learning-infused control.

**Table 8.** Performance Evaluation during Two-Phase Fault

Performance Indicator (%)	No Controller	Resistance-Based FCL	Conventional FCL	Series Dynamic Braking Resistor (SDBR)
Terminal Voltage	3.0487	0.4907	0.516	0.7203
Terminal Current	13.9988	1.8782	1.6969	4.4457
Terminal Speed	0.0784	0.0399	0.0403	0.0412
Active Power	1.5868	0.9163	1.0182	1.0308
DC Link Voltage	0.6133	0.1355	0.3282	0.5105

Table 8 extends the analysis to a two-phase fault scenario, which presents its own challenges to system stability. Similar to the previous tables, it provides a comparative assessment of different control methods:

**Interpretation of Table 8:** In the presence of two-phase faults, the proposed resistance-based FCL continues

to excel. It effectively limits fault currents, as evidenced by reductions in terminal current and active power. Terminal voltage, terminal speed, and DC link voltage are well-maintained, highlighting the robustness of the deep learning-driven control strategy.

**Table 9.** Performance Evaluation during Single-Phase-to-Ground Fault

Performance Indicator (%)	No Controller	Resistance-Based FCL	Conventional FCL	Series Dynamic Braking Resistor (SDBR)
Terminal Voltage	2.1779	0.2063	0.4791	0.514
Terminal Current	14.381	0.6254	0.6478	1.0805
Terminal Speed	0.0429	0.0222	0.0231	0.0226
Active Power	1.2706	0.4432	0.4805	0.5671
DC Link Voltage	0.1609	0.0544	0.0595	0.0637

Table 9 delves into a single-phase-to-ground fault scenario, highlighting the impact of different control methods on system behavior:

**Interpretation of Table 9:** The single-phase-to-ground fault scenario reveals the proposed resistance-based FCL's capability to control fault currents effectively. It ensures terminal voltage stability and manages terminal current within acceptable levels. The deep learning-integrated control maintains the system's stability, underscoring its superior performance.

The tables collectively demonstrate that the proposed resistance-based FCL, integrated with deep learning techniques, outperforms other control strategies. By effectively managing fault currents and maintaining system parameters within the 10%± range of their initial values, it enhances the transient stability of DFIG-based wind turbine systems. These tables serve as a valuable resource for researchers and engineers, enabling them to make informed decisions about the most suitable control strategies for specific fault scenarios.

## 6. Conclusion

In the realm of renewable energy, the reliability of power grids remains a significant challenge. Doubly Fed Induction Generators (DFIGs) with advanced power converters have gained prominence in the wind energy market. However, the need for DFIG systems to ensure transient stability during grid disturbances is pressing. Previous research has shown that conventional DFIG control tools fall short in maintaining transient stability across various fault scenarios. This underscores the importance of integrating novel external tools to comprehensively safeguard stability. This study introduces a pioneering approach to enhance transient stability in DFIG-based wind energy systems. A resistance-based fault current limiter is proposed to transform transient stability dynamics within these systems. The results confirm its efficacy in mitigating voltage and current overshoot during faults, a crucial factor in maintaining operational integrity. As the renewable energy era progresses, this research underscores the growing significance of advanced control

strategies and auxiliary tools. The integration of such innovations is crucial to ensuring the continued growth and dependability of wind energy within the global power landscape. As we move forward, integrating deep learning techniques promises to further enhance control strategies and tools. By infusing intelligent decision-making and adaptability, deep learning will play a pivotal role in advancing transient stability in DFIG-based wind energy systems, accelerating the transition to sustainable power generation.

## REFERENCES

- [1] S. Alaraifi, M. S. El Moursi, and H. H. Zeineldin, "Optimal allocation of HTS-FCL for power system security and stability enhancement," *IEEE Transactions on Power Systems*, vol. 28, no. 4, pp. 4701–4711, 2013.
- [2] A. Rahdan and A. Khaleghi, "Phasor measurement units allocation against load redistribution attacks based on Greedy algorithm," *Advances in Engineering and Intelligence Systems*, vol. 2, no. 03, 2023.
- [3] P. M. Anderson and A. A. Fouad, *Power system control and stability*. John Wiley & Sons, 2008.
- [4] C. A. Baldan, C. Y. Shigue, J. S. Lamas, and E. Ruppert Filho, "Test results of a superconducting fault current limiter using YBCO coated conductor," *IEEE transactions on applied superconductivity*, vol. 17, no. 2, pp. 1903–1906, 2007.
- [5] S. M. Blair, C. D. Booth, and G. M. Burt, "Current-time characteristics of resistive superconducting fault current limiters," *IEEE transactions on applied superconductivity*, vol. 22, no. 2, p. 5600205, 2012.
- [6] S. M. Blair, "The analysis and application of resistive superconducting fault current limiters in present and future power systems," 2013.
- [7] A. Khaleghi, M. S. Ghazizadeh, M. R. Aghamohammadi, J. M. Guerrero, J. C. Vasquez, and Y. Guan, "A Probabilistic Data Recovery Framework against Load Redistribution Attacks Based on Bayesian Network and Bias Correction Method," *IEEE Transactions on Power Systems*, 2023.
- [8] L. Chen *et al.*, "Technical evaluation of

- superconducting fault current limiters used in a micro-grid by considering the fault characteristics of distributed generation, energy storage and power loads,” *Energies (Basel)*, vol. 9, no. 10, p. 769, 2016.
- [9] D. Das, *Electrical power systems*. New Age International, 2007.
- [10] M. S. Ghazizadeh and M. R. Aghamohammadi, “A deep learning-based attack detection mechanism against potential cascading failure induced by load redistribution attacks,” *IEEE Trans Smart Grid*, 2023.
- [11] S. Eckroad, “Superconducting fault current limiters,” *Electric power research institut*, vol. 1017793, 2009.
- [12] M. Rajabzadeh and M. Kalantar, “Enhance the resilience of distribution system against direct and indirect effects of extreme winds using battery energy storage systems,” *Sustain Cities Soc*, vol. 76, p. 103486, 2022.
- [13] J. D. Glover, T. J. Overbye, and M. S. Sarma, *Power system analysis & design*. Cengage Learning, 2017.
- [14] L. L. Grigsby, *Power system stability and control*. CRC press, 2007.
- [15] A. Jain, V. K. Dubey, G. Jawale, H. A. Mangalvedekar, and K. Kanakgiri, “Limiting fault current in a power system network by SFCL: A step input approach,” in *2016 IEEE 6th International Conference on Power Systems (ICPS)*, IEEE, 2016, pp. 1–5.
- [16] M. A. Kamarposhti, H. Shokouhandeh, I. Colak, S. S. Band, and K. Eguchi, “Optimal location of FACTS devices in order to simultaneously improving transmission losses and stability margin using artificial bee colony algorithm,” *IEEE Access*, vol. 9, pp. 125920–125929, 2021.
- [17] M. Khatibi and M. Bigdeli, “Transient stability improvement of power systems by optimal sizing and allocation of resistive superconducting fault current limiters using particle swarm optimization,” *Advanced Energy: An International Journal (AEIJ)*, vol. 1, no. 3, pp. 11–27, 2014.
- [18] S. Kodle, V. Padmini, H. J. Bahirat, S. A. Khaparde, P. Lubicki, and V. Dabeer, “Application of Super Conducting fault current limiter in Indian grid,” in *2016 IEEE 6th International Conference on Power Systems (ICPS)*, IEEE, 2016, pp. 1–6.
- [19] L. Kovalsky, X. Yuan, K. Tekletsadik, A. Keri, J. Bock, and F. Breuer, “Applications of superconducting fault current limiters in electric power transmission systems,” *IEEE Transactions on Applied Superconductivity*, vol. 15, no. 2, pp. 2130–2133, 2005.
- [20] T. Koyama and S. Yanabu, “Study and development of superconducting fault current limiter with high speed reclosing,” *IEEE transactions on applied superconductivity*, vol. 19, no. 3, pp. 1868–1871, 2009.
- [21] M. Rajabzadeh and M. Kalantar, “Improving the resilience of distribution network in coming across seismic damage using mobile battery energy storage system,” *J Energy Storage*, vol. 52, p. 104891, 2022.
- [22] P. Kundur *et al.*, “Definition and classification of power system stability IEEE/CIGRE joint task force on stability terms and definitions,” *IEEE transactions on Power Systems*, vol. 19, no. 3, pp. 1387–1401, 2004.
- [23] P. Kundur, “Power system stability,” *Power system stability and control*, vol. 10, pp. 1–7, 2007.
- [24] A. Khaleghi, M. S. Ghazizadeh, M. Aghamohammadi, J. M. Guerrero, J. C. Vasquez, and Y. Guan, “A defensive mechanism against load redistribution attacks with sequential outage potential using encrypted PMUs,” in *IECON 2023-49th Annual Conference of the IEEE Industrial Electronics Society*, IEEE, 2023, pp. 1–6.
- [25] G.-J. Lee and A. Luiz, “Superconductivity application in power system,” in *Applications of high-Tc superconductivity*, Intech, 2011, pp. 45–74.
- [26] D. A. L. Roca, P. Mercado, and G. Suvire, “System frequency response model considering the influence of power system stabilizers,” *IEEE Latin America Transactions*, vol. 20, no. 6, pp. 912–920, 2022.